

Communication

Atomic pairwise distribution function analysis of the amorphous phase prepared by different routes

J. P. Bøtker^{1*}, V. Koradia¹, M. Savolainen¹, T. Rades², J. Rantanen¹

¹Faculty of Pharmaceutical Sciences, University of Copenhagen, Universitetsparken 2, 2100 Copenhagen, Denmark

²School of Pharmacy, University of Otago, 18 Frederick Street, Dunedin 9054, New Zealand

Emails: jpb@farma.ku.dk, vishal.koradia@novartis.com, msa@farma.ku.dk,

thomas.rades@otago.ac.nz, jtr@farma.ku.dk

Vishal Koradia's current address is Technical R&D, Novartis Pharma AG, Basel, CH-4056,

Switzerland

* Author to whom correspondence should be addressed; Tel.: +45 35 33 60 00

Received: / Accepted: / Published:

Abstract: Amlodipine besilate, a calcium channel antagonist, exist in several solid forms. The anhydrate and dihydrate forms are in focus in this study. Milling was performed on the anhydrate form whereas the dihydrate form was subjected to quench cooling thereby creating amorphous materials from both the starting forms. The milled and quench cooled samples together with the crystalline starting materials were analyzed with X-ray powder diffraction (XRPD), Raman spectroscopy and atomic pair-wise distribution function (PDF) analysis of the XRPD data. The PDF analysis was superior in displaying differences between the amorphous samples prepared by milling or quench cooling compared to XRPD raw data and Raman spectroscopy.

Keywords: atomic pair wise distribution functions; Raman spectroscopy; XRPD; Amlodipine besilate.

1. Introduction

The amorphous state of solid compounds is characterized by the absence of orientational and positional long range order, typical for the crystalline solid state. Amorphous forms may however contain some residual order from their crystalline counterparts (especially when prepared by a milling process) as well as near order over the length scale of a few molecules. Amorphous forms of drugs are attractive in drug development, especially for poorly water soluble compounds (BCS class 2 and 4 compounds), as they possess a faster dissolution rate than their respective crystalline forms. This advantage however, goes hand in hand with an increased physical instability, and amorphous systems have a tendency to convert back to the thermodynamically more stable crystalline state (either a metastable or the stable polymorphic form). In this work amlodipine besilate was either milled or quench cooled, which in both circumstances yielded an x-ray amorphous system (x-ray amorphous is defined here as the visual absence of diffractions in the diffractograms). Although conventional x-ray powder diffraction (XRPD) is routinely used to analyze non-crystalline material it has to be taken into account that the technique is directly measuring a crystalline property (long range order, leading to diffractions in the diffractograms), the absence of which is in turn interpreted as amorphousness. In contrast, the application of atomic pair-wise distribution functions (PDF) to the diffractograms takes both, diffracted and diffuse x-ray scattering into account, and thus also probes the non-crystalline signals of the diffractograms.¹

The PDF technique utilizes a Fourier transformation of the XRPD diffractogram to produce a trace in a coordinate system. The y-axis in the PDF trace is corresponding to the probability of finding two atoms separated by a distance stipulated by the x-axis. The PDF hence assesses the inter-atomic distances of the material.^{1,2}

2. Experimental section

Amlodipine besilate (AMB) was used as a model active pharmaceutical ingredient (API). The anhydrate form of AMB (AH) was used as received. The dihydrate form (DH) was prepared from an aqueous slurry by stirring the AH crystals in water for 2 days at 25 °C. The crystals were collected by filtration and dried at 40 °C.³ Amorphous AMB (AM) forms were prepared by the following methods: The DH form was heated to 106 °C and subsequently underwent dehydration. The molten phase obtained by dehydration was quench cooled to obtain amorphous AM form. Milling of AH was done with a ball mill (Retsch MM 400, Germany) with two 25 mL jars containing 400 mg of AH and two 9 mm steel beads. Milling was performed for 60 min at a milling frequency of 25 Hz. The products were analyzed using X-ray powder diffraction (XRPD) and Raman spectroscopy. XRPD data were subjected to PDF analysis using Fourier transformation thereby obtaining residual long range order information.

Multivariate data analysis (MVDA)

Multivariate data analysis was performed using principal component analysis (PCA). Before PCA, standard normal variant (SNV) transformation was performed to remove intensity differences unrelated to the sample composition and the spectra were then mean centered. PCA, preprocessing and scaling were performed using PLS toolbox version 6.0.1 (Eigenvector Research Inc., Wenatchee, WA, USA) installed on Matlab version 7.11.0.584 2010b (Natick, Massachusetts, USA) .

Raman spectroscopy

The two solid forms as well as the changes in the solid samples after processing were analyzed using a Raman spectrometer (Control Development Inc., South Bend, IN, USA) equipped with a thermoelectrically cooled CCD detector and a fiber optic probe (InPhotonics, Norwood, MA, USA). The measurements were carried out at room temperature using a 500 mW laser source with a wavelength of 785 nm (Starbright 785S, Torsana Laser Technologies, Skodsborg, Denmark). The integration time was 3 s and each spectrum was an average of 8 scans.

XRPD

X-ray powder diffractograms were measured on a PANalytical X'Pert Pro θ/θ diffractometer equipped with a PIXcel detector (PANalytical B.V., Almelo, The Netherlands). A continuous 2θ scan was performed in a range of 2° to 40° using $\text{CuK}\alpha$ radiation ($\lambda = 1.5406 \text{ \AA}$) with as step size of $0.0390^\circ 2\theta$. The $\text{K}\beta$ radiation was eliminated by a nickel filter. The voltage and current applied were 45 kV and 40 mA respectively. The film sample was placed in a 0.2 mm deep sample holder and the measurement was performed at ambient conditions. Data were collected using X'Pert data collector version 2.2 and were analyzed with X'Pert highscore plus version 2.2.4 (both from PANalytical B.V., Almelo, The Netherlands).

Atomic pair wise distribution function (PDF)

Atomic pair-wise distribution function (PDF) analysis was performed by Fourier transforming the XRPD diffractograms using the freeware program RAD developed by V. Petkov at the University of Sofia, Department of Solid State Physics, Sofia-1126, Bulgaria. The setup for the program is described elsewhere.⁴ The program can be downloaded at this site: <http://www.pa.msu.edu/~petkov/software.html> (accessed 1st of October 2010).

3. Results and discussion

The different forms of AMB were subjected to X-ray powder diffraction. The milled samples of AH (M1, M2 and M3) as well as the quench cooled samples of DH (Q1, Q2 and Q3) displayed XRPD diffractograms that can be characterised as broad and featureless whereas the crystalline anhydrate (AH) and dihydrate (DH) show diffractions which are in accordance with the literature³ (Figure 1). The broad features seen for the processed samples do not provide any visual evidence for differences in the degree of disorder between the milled and quench cooled samples.

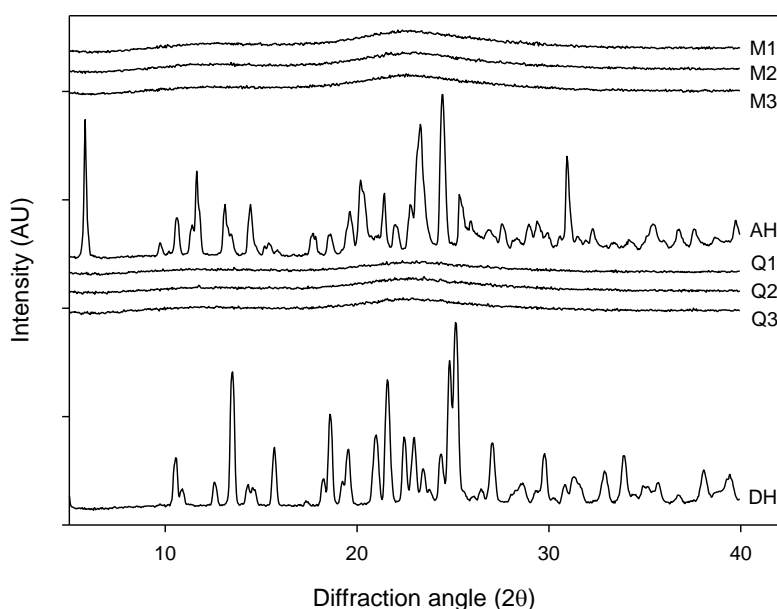


Figure 1 XRPD diffractograms of: milled samples (M1, M2 and M3), Quench cooled samples (Q1, Q2 and Q3), crystalline anhydrate (AH) and crystalline dihydrate (DH).

MVDA was utilized to try and elucidate any differences in the diffractograms (Figure 2). The model explained 93.7% of the variation in the data set using two principal components. The only obtainable information from this score plot is that the crystalline counterparts can be readily distinguished from one another and the processed samples. However, such information is easily obtained from the diffractograms themselves. Several other models using different preprocessing and multiple principal components were tried. However it was not possible to obtain a discriminative power of the XRPD diffractograms between the milled and quench cooled samples.

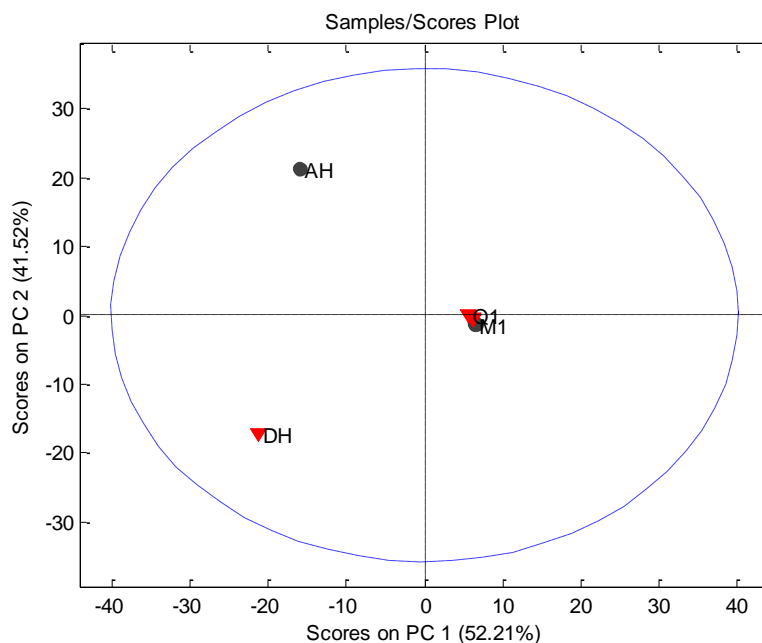


Figure 2 PCA score plot of XRPD data of milled samples (M1, M2 and M3), Quench cooled samples (Q1, Q2 and Q3), crystalline anhydrate (AH) and crystalline dihydrate (DH).

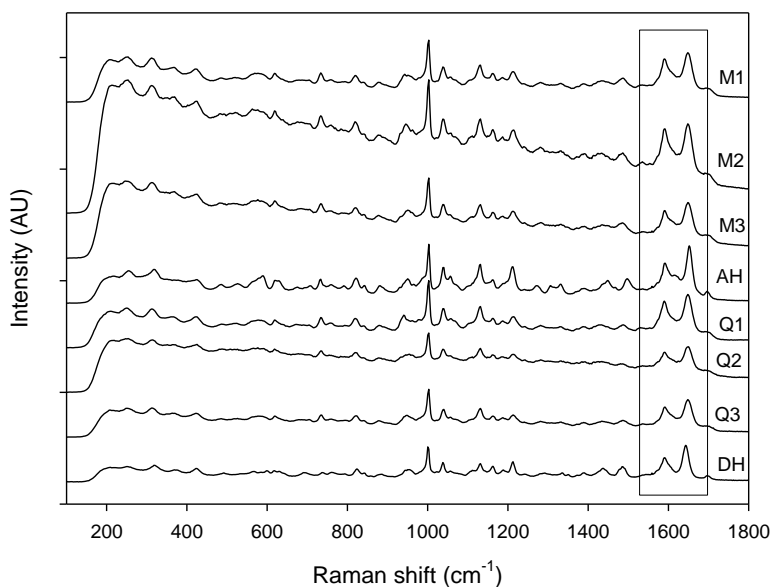


Figure 3 Raman spectra of milled samples (M1, M2 and M3), Quench cooled samples (Q1, Q2 and Q3), crystalline anhydrate (AH) and crystalline dihydrate (DH).

Figure 3 shows that a change could be noted in the Raman spectra for the milled and quench cooled samples compared to the original crystalline forms. For example, a peak shift from 1643 cm^{-1} to 1648 cm^{-1} occurred during dehydration and a peak shift from 1652 cm^{-1} to 1648 cm^{-1} occurred during milling (red line, Figure 4). This peak at 1648 cm^{-1} corresponds to the amorphous form and can be used to monitor the solid state transformation.

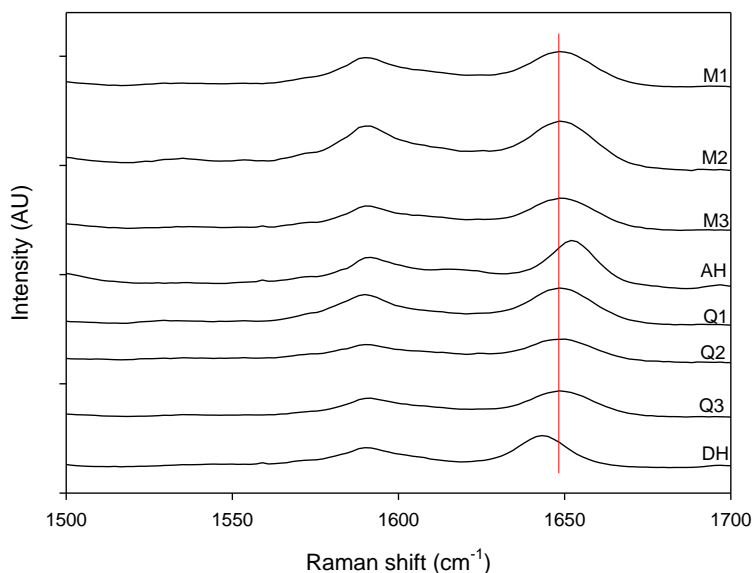


Figure 4 Magnification of the 1500 cm^{-1} to 1600 cm^{-1} spectral region. Milled samples (M1, M2 and M3), Quench cooled samples (Q1, Q2 and Q3), crystalline anhydrate (AH) and crystalline dihydrate (DH).

PCA, using two principal components explaining 88.85% of the variation in the spectral region 80 cm^{-1} to 1800 cm^{-1} , was utilized with SNV and mean centering as preprocessing, to try and elucidate any differences in the Raman spectra. However, as seen in Figure 5 no differences could be readily extracted from the processed samples using the two first components. It is seen that two separate groups are formed, but each group contains samples from both the milled and quench cooled process

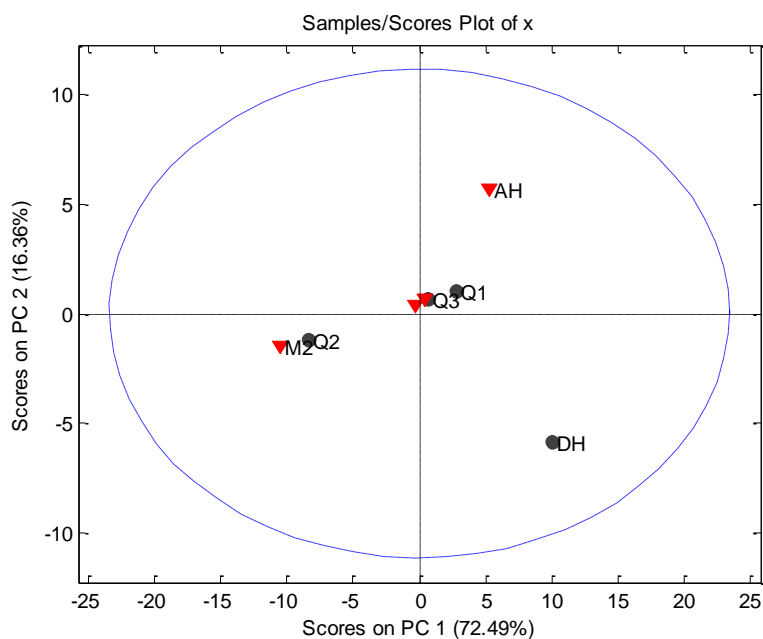


Figure 5 PCA score plot of Raman data PC1 vs. PC2. Milled samples (M1, M2 and M3), Quench cooled samples (Q1, Q2 and Q3), crystalline anhydrate (AH) and crystalline dihydrate (DH).

The PDF of the XRPD data displayed in figure 6 represents the various milled and dehydrated samples as well as the crystalline DH and AH starting material. The value of the y-axis in the PDF trace is corresponding to the probability of finding two atoms separated with the distance stipulated by the x-axis. The peaks in the PDF trace are therefore represent the average inter-atomic distances in the material. It is observed that the PDF trace of all the samples attenuates with varying rates towards unity at distances far away from the origin. Furthermore, it is observed that the crystalline AH and DH starting material has an attenuation in the peaks that is much slower than the corresponding attenuation of the processed samples.

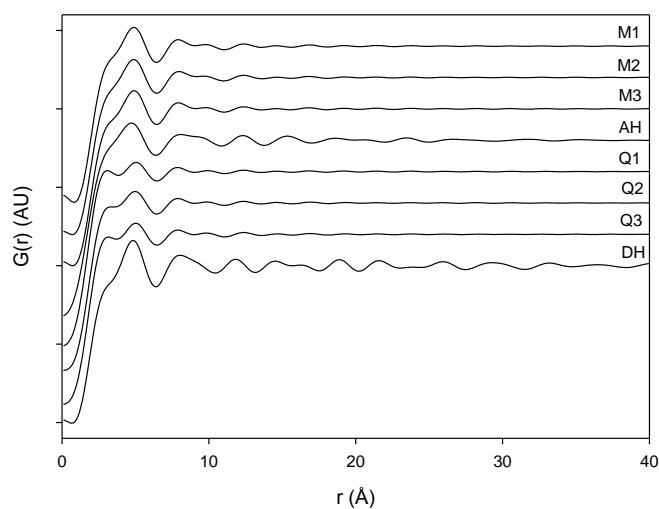


Figure 6 PDF pattern of the Milled samples (M1, M2 and M3), Quench cooled samples (Q1, Q2 and Q3), crystalline anhydrate (AH) and crystalline dihydrate (DH).

When overlaying the milled samples (black lines) and quench cooled samples (red lines) in Figure 7 it is observed that there is a lower value of the peaks for the quench cooled samples than for the milled samples which indicates a higher degree of disorder in the quench cooled samples.

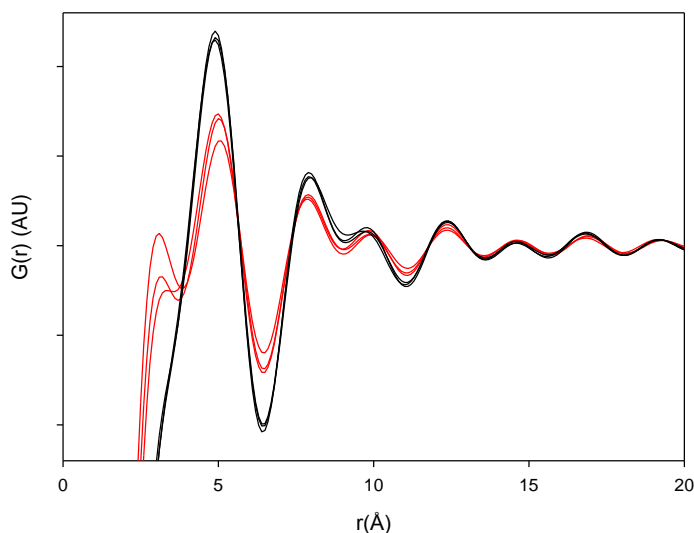


Figure 7 PDF patterns of the processed samples. Milled samples: black lines and quench cooled samples: red lines

PCA was carried out on the PDF data in the interval 4 Å to 40 Å to assess the structural disorder induced by milling or quench cooling. The PCA plot in figure 10 utilized 2 principal components to explain 89.76 % of the variation. It is observed that the crystalline samples were separated in the score plot from the processed samples and that the milled and quench cooled samples are separated from one another (Figure 8). The score plot is using principal component 1 to separate the samples according to disorder and hence lowered peak values which are also seen from the loading vector of principal component 1 (Figure 9). Principal component 2 is separating the crystalline starting materials.

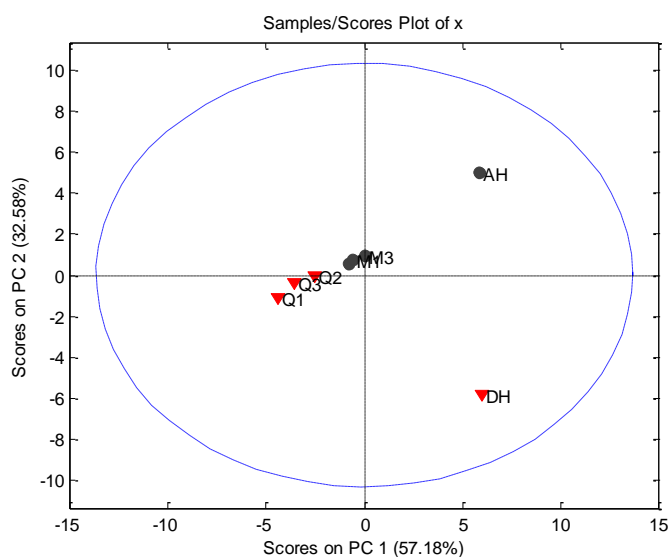


Figure 8 PCA score plot of PDF data PC1 vs. PC2 Milled samples (M1, M2 and M3), Quench cooled samples (Q1, Q2 and Q3), crystalline anhydrate (AH) and crystalline dihydrate (DH).

These differences in principal component 1 also suggest that the residual long range order is the lowest for the quench cooled samples since they are situated furthest away from the crystalline starting material. Finally, it should also be emphasized that the loading vector for the first principal component has a sensible meaning when one is comparing it to the raw data, which was not the case for the Raman data (Figure 9).

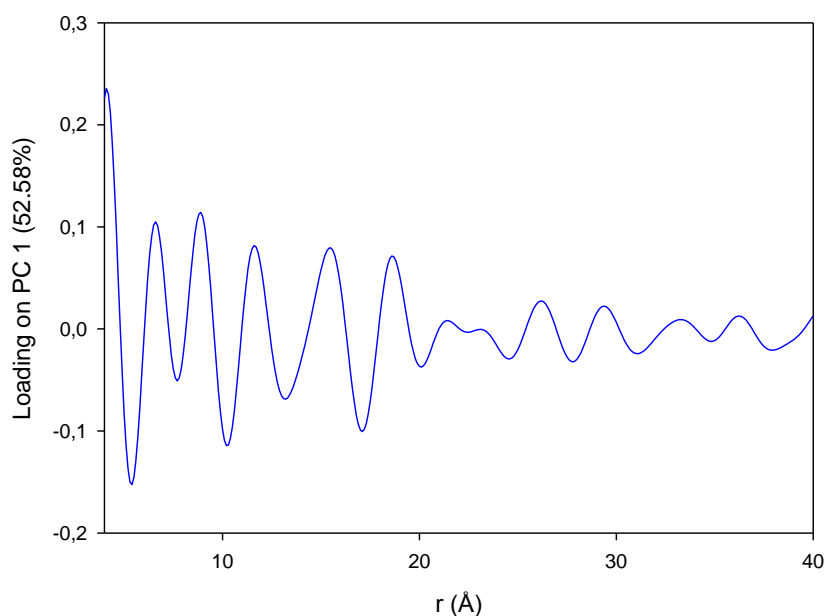


Figure 9 Loading vector for the PC1 of the PDF data.

4. Conclusion

It is shown that atomic pair-wise distribution function (PDF) analysis of the XRPD data provided a possibility to discriminate between milled samples, quench cooled samples and the starting crystalline materials, whereas X-ray powder diffraction data as such or Raman spectroscopy were not capable of separating these two preparational routes. PDF analysis may therefore be utilized to obtain a deeper understanding of the amorphous state.

References and Notes

1. Bates, S.; Zograf, G.; Engers, D.; Morris, K.; Crowley, K.; Newman, A. Analysis of amorphous and nanocrystalline solids from their X-ray diffraction patterns. *Pharmaceutical Research* **2006**, *23*, (10), 2333-2349.
2. Dinnebier, R. E.; Billinge, S. J. L., *Powder diffraction : theory and practice*. ed.; Royal Society of Chemistry: Cambridge, 2008; 'Vol.' p xxi, 582 p.

3. Koradia, V.; de Diego, H. L.; Frydenvang, K.; Ringkjøbing-Ellema, M.; Mullertz, A.; Bond, A. D.; Rantanen, J. Solid Forms of Amlodipine Besylate Physicochemical, Structural, and Thermodynamic Characterization. *Crystal Growth & Design* **2010**, *10*, (12), 5279-5290.
4. Petkov, V. Rad, a Program for Analysis of X-Ray-Diffraction Data from Amorphous Materials for Personal Computers. *J Appl Crystallogr* **1989**, *22*, 387-389.